Scales of Thermal Variability in the Tropical Pacific

T. P. BARNETT AND W. C. PATZERT

Scripps Institution of Oceanography, La Jolla, CA 92093

(Manuscript received 8 October 1979, in final form 4 December 1979)

ABSTRACT

Long-range P-3 aircraft have been used to occupy two 4000 km long sections from 20°N to 17°S along 150 and 158°W in the central equatorial Pacific. The temperature field along these sections was measured at approximately weekly intervals for three months (November 1977–January 1978). The principal meridional scales of variability derived from this data set suggest highly coherent fluctuations in the upper ocean thermal structure within ±10° of the equator. The region of coherent variability extends across the equator, across boundaries of major current systems and through the ITCZ. The time scale of these fluctuations is of order 2–3 months. Variability in the zonal direction is also coherent, although of smaller amplitude, with space scales of at least 2000 km and time scales of several months. These latter modes of variability are suggestive of propagating disturbances, although that hypothesis could not be proved with the current data set. The observed oceanic variability at 150°W was not closely related with changes in the local wind stress or curl of the wind stress field in the central tropical Pacific, suggesting that a large part of the observed oceanic fluctuations may not have been "locally" forced.

The relation between transports in the North Equatorial Countercurrent derived from the AXBT data and *T/S* relations agreed well with similar transport estimates obtained from hydrographic observations and current meter arrays. This suggests that the scales of variability we have observed in the temperature field may also apply, in part, to the zonal velocity and transport fields.

1. Introduction

As a component in the Global Weather Experiment, North Pacific Experiment (NORPAX) scientists are just beginning a large-scale long-term field experiment in the central tropical Pacific. The prime focus of this experiment is to further examine the nature of and mechanisms responsible for the large climatological variations observed in the equatorial ocean and atmosphere. However, before such an ambitious experiment could be fully designed and initiated it was important to know the space and time scales of natural variability in the region. With this information, proper sampling schemes could be identified and implemented. Measurements were made from ships, aircraft, moored instrumentation, satellite-tracked drifting buoys and island stations. Each of the data sets provided crucial information describing oceanic variability. In the present paper we report the typical space and time scales that were found in the thermal structure of the central equatorial Pacific between 20°N and 17°S during the winter 1977–78.

Previous scale studies in the equatorial Pacific Ocean have been relatively few. Some work has been done on the correlation between sea level gages located on islands of differing separations (e.g., Roden, 1963; Wyrtki, 1978a). Also, some preliminary estimates of variability in the thermal structure have been obtained (e.g., Austin, 1960; Wyrtki *et al.*, 1977; Meyers, 1978, 1979). Some estimate of the variation in the equatorial surface current systems (Wyrtki, 1978b; Legeckis, 1977) as well as the deeper waters beneath the equatorial currents (Harvey and Patzert, 1976) have been made.

In the present work we concentrate on the variability in the near-surface temperature field. Studies of such variability have been attempted previously by Wyrtki *et al.* (1977) and Hires and Montgomery (1972). However, in both cases the data were taken from relatively slow-moving ships and at rather irregular space and (particularly) time intervals. Thus the studies may well have missed considerable large-scale variability or, worse yet, been aliased.

In our experiment, repeated deployments of airborne expendable bathythermographs (AXBT's) from long-range P-3 aircraft were made between latitudes 20°N–17°S along meridians at 150 and 158°W. This program was much like that called for by Montgomery (1969). Each meridional section was occupied on an approximately weekly basis, although early in the experiment a series of "burst sampling" flights was carried out to estimate the strength of variations with time scales of several days. In the subsequent sections of the paper we describe the experimental plan, instruments, analysis technique and then the scales of meridional and longitudinal variability that were observed. Final sections at-

0022-3670/80/040529-12$07.00

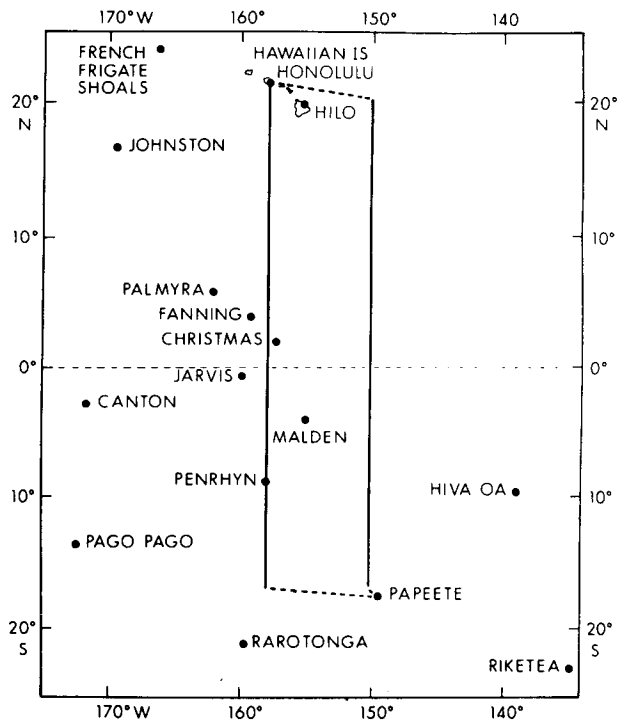

FIG. 1. Location map. The heavy black lines indicate the meridional sections that were occupied during this experiment. NORPAX sea level stations are also indicated.

tempt to relate variations in the wind field with the observed variations in the ocean temperature field and to show that the temperature fluctuations are probably closely related to large-scale changes in the current systems.

2. The data

The experimental plan called for us to make round trip flights once per week between Honolulu and Tahiti (Fig. 1). During the southbound flight, along the 150th meridian, vertical temperature profiles were taken by AXBT's (see below) at every 1° of latitude except between 14°N and 7°S where instruments were dropped every 0.5°. After a day layover in Tahiti (for rest), a return leg was flown, beginning at 17°S, up the 158th meridian to Honolulu. The sampling interval was the same as along 150°W. This round trip was carried out weekly during the months of December 1977 and January 1978. The 150° section alone was occupied during the month of November. By concentrating on this single meridian we could occupy the section intensively to investigate the relative importance of shorter term fluctuations to our measurement program, e.g., the 4-day waves that have been discussed previously in the literature (cf. Groves, 1956; Wunsch and Gill, 1976).

Airborne expendable bathythermographs were our principal measurement tools. They are launched from the aircraft, descend to the water surface where a probe is released from the drifting portion of the AXBT. As a probe falls it sends back information on the temperature structure (via hard wire) that is used to modulate a radio signal from the surface buoy. The signal is received in the aircraft and the modulation frequency stripped from the carrier. This frequency was eventually translated into temperature information. The AXBT's used in this experiment come from a single manufacturer's production lot. We selected 10% of the lot at random and calibrated each of the (150) instruments. The results of these calculations confirm that the previously determined relation between frequency f (Hz) and temperature T (°C), i.e.,

$$T = -38.333 + 0.026899f,$$

was valid for the instruments used in this experiment to an accuracy of ±0.2°C. At-sea tests also confirmed the laboratory results that these AXBT's do not suffer the thermal lag problem discovered in earlier AXBT's (Sessions and Barnett, 1980). Thus, we conclude that the instruments used in this experiment had an absolute accuracy of ±0.2°C. Comparisons with CTD observations taken from the R/V *Kana Keoki* during the experiment when aircraft and ship tracks coincided support this conclusion, although there was a slight tendency for the AXBT's to report isotherm depths that were more shallow than the CTD. The average of this bias was 7 m, a value that was independent of depth and current regime. A cross comparison of XBT and AXBT isotherm depths showed the two measurement systems gave virtually identical results. Since we are working here with variations within the AXBT data set only, the small CTD/AXBT differences will not affect our conclusions.

A total of 1572 BT traces were obtained during the course of the experiment. Each trace was scrutinized by a series of computer algorithms to detect any potential sources of error, e.g., signal dropout. In addition each trace was visually scrutinized on a cathode ray tube to pick up any peculiarities that the computer checks missed. Less than 1% of the data collected required any type of correction. A typical section resulting from one of the flights is shown in Fig. 2. Additional sections are displayed by Patzert *et al.* (1978), a data report which also describes experimental procedures in detail.

The general properties of the data fields that we obtained are shown in Figs. 3 and 4. The first panels show the mean field estimated for the duration of the experiment along each meridian. The characteristic features of the equatorial circulation system clearly manifest themselves (cf. Wyrtki *et al.*, 1977). A strong ridge in the thermal structure near 10°N acts as a dividing line between the North Equatorial Current (NEC) to the north and the North

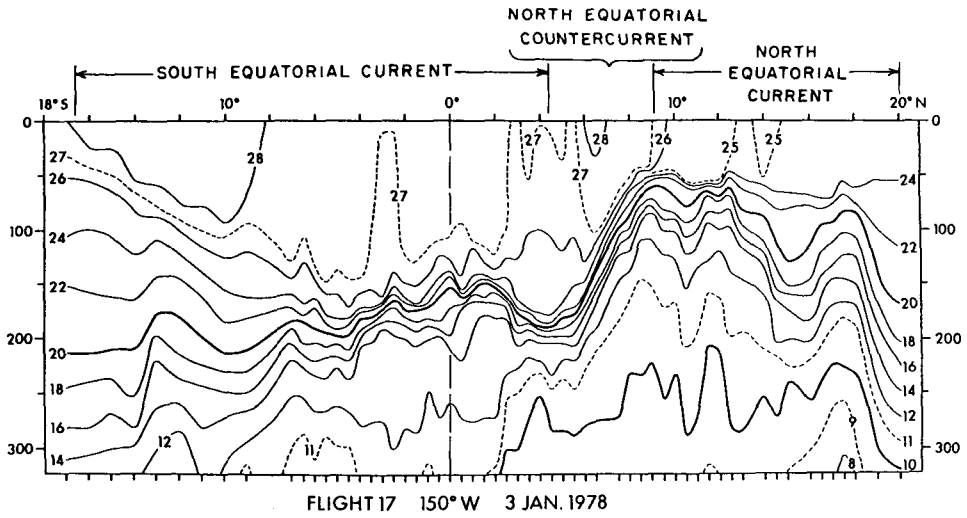

FIG. 2. A typical meridional section of temperature (°C).

Equatorial Countercurrent (NECC) to the south. The trough near 4°N marks the southern boundary of the North Equatorial Countercurrent with the South Equatorial Current (SEC) to the south. The characteristic spreading of the isotherms in the vicinity of the equator shows the existence of the Equatorial Undercurrent in the thermocline and upwelling above.

The variability associated with the mean field is shown in the lower panels of Figs. 3 and 4. In terms of standard deviations we see, as expected, that the highest values are generally in the regions of highest temperature gradient. The variability decreases at both the northern and southern ends of the sections as the vertical gradients become less intense. The shape of the major variance patterns shown in this illustration cut across current boundaries, the equator, and even the position of the Intertropical Convergence Zone (ITCZ). It will be well to bear this fact in mind, as well as the general shape of the regions of high variance, for they will play a major part in the conclusions that we develop below.

Another view of the data is given by the standard deviations of isotherm displacements about mean isotherm depths for the 14–25°C temperatures

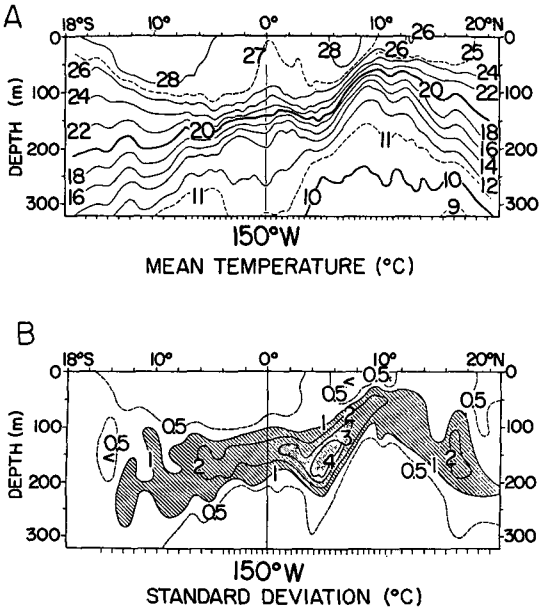

FIG. 3. Mean field (A) and standard deviation about the mean (B) observed over the duration of the experiment at 150°W.

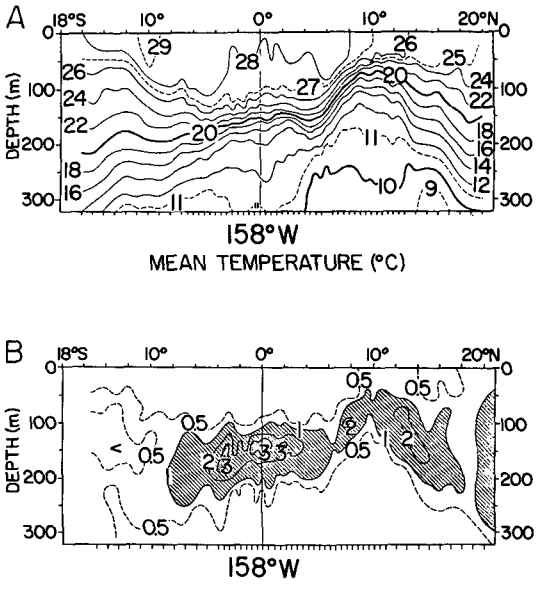

FIG. 4. As in Fig. 3 except at 158°W.

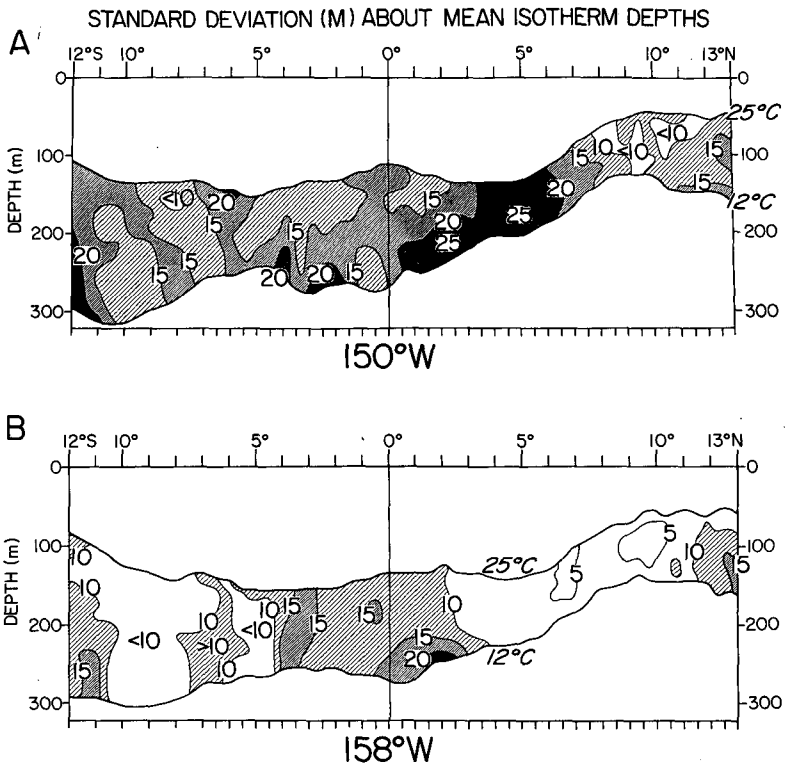

FIG. 5. Standard deviation of isotherm depths (m) plotted at the mean isotherm depth for the 25–12°C temperatures for 150 and 158°W.

(Fig. 5). for reasons which will become clear in the next section we concentrate on the near equatorial latitude band between ±12°. The greatest variability occurs in the NECC region. Over most of the middle and southern parts of the sections the variability is slightly higher at depth. Note the striped nature of the isotherm depth fluctuation and the fact that the 150°W section has about twice the variability of the 158°W section.

3. Analysis method

Nearly one-half million data points were collected during the course of the airborne experiment. Together they represent the field of temperature $T(y,z,t)$ where y is the meridional direction, z depth and t time, along each of two meridians. To extract the pertinent information from this large data set we have reduced it to a set of empirical orthogonal functions (EOF's) so that the temperature field is represented by a relatively few of its normal modes of variability, i.e.,

$$T(\mathbf{x},t) = \sum_{l=1}^{p} A_l(t)B_l(\mathbf{x}), \qquad (1)$$

where $\mathbf{x} = (y,z)$. Note this analysis technique is not affected by spatial inhomogeneity as would be, say, a traditional scale length analysis using correlation functions. The B_l are the eigenvectors of the covariance matrix

$$\Phi(\mathbf{x},\mathbf{x}') = (n-1)^{-1} \sum_{t=1}^{n} T(\mathbf{x},t)T(\mathbf{x}',t) \qquad (2)$$

and describe patterns of covariability in the T-field. The $A_l(t)$ are the time-dependent amplitude functions that modulate these principal patterns. Since $\langle B_l \cdot B_m \rangle = \delta_{lm}$ it may be shown that $\langle A_l A_m \rangle_t = \lambda_l \delta_{lm}$, where λ_l is the lth eigenvalue of Φ, δ_{lm} is the Kronecker delta and the $\langle \cdots \rangle_t$ denote a time average.

The eigenvalues associated with the B_l have a property that

$$\sum_{l=1}^{p} \lambda_l = (n-1)^{-1} \sum_{t=1}^{n} \sum_{\mathbf{x}=1}^{m} T^2(\mathbf{x},t),$$

so that the ith pattern accounts for a fraction of the total field variance given by $\lambda_i / \sum_l \lambda_l$.

Note that for fixed λ_l, the $B_l(\mathbf{x})$ describe the spatial distribution of covariance in the temperature field. Thus, regions of positive and negative values for components of a selected B_l indicate variability that is temporally coherent but of opposite phase, e.g., one region is warm when the other region is cool. This interpretation of the B_l is important to bear in mind in the following sections. Also to help the reader

we have renormalized the B_l so that $\langle B_l B_m \rangle = \lambda_l \delta_{lm}$, where values of B_l now carry units of °C. This required a renormalization of A_l so that $\langle A_l A_m \rangle_t = \delta_{lm}$.

A set of statistical filtering rules has been developed (Preisendorfer and Barnett, 1977) to select from the EOF analysis, via the λ_l, the patterns that differ significantly from those expected from a field of randomly distributed variates. The filter consists of comparing the eigenvalues (λ_l) of the data field with those (λ_l') expected from a comparable field of Gaussian random variates. The mode number p', where the λ_l becomes statistically equal to the λ_l', provide us with a "stopping" rule. We thus ignore modes greater than p' since their energy is indistinguishable from that of a purely random field. In the present study we generally found $p' = 2$ for most of the EOF runs and therefore called higher modes "noise". In general, the first two modes accounted for roughly 50–70% of the observed variance.

4. Meridional scales of variability

The principal scales of variability along 150 and 158°W were derived from the EOF's of the section time series. These patterns of covariability are shown in Figs. 6 and 7 for the first two eigenmodes. Also shown are the corresponding time-dependent amplitude functions.

A number of conclusions may be drawn from these illustrations:

1) The first two modes for thermal variability along 150 and 158°W account for 67 and 54% of the variance, respectively. Application of the filtering rule (cf. Section 3) to the eigenvalues associated with modes higher than 2 show these modes to be not significantly different from those expected from a purely random process. Thus the principal information in the data set is contained in the first two modes along each section.

2) Coherent variability exists in the 150°W section from 10°S to 14°N. The variability is centered principally on the region of most intense thermal gradient. The near-surface thermal structure over this 24° of latitude fluctuates largely in unison. The second mode of the variability along this meridian shows a region of coherent fluctuation within ±4° of the equator, accompanied by a region extending from 4 to 10°N, wherein the variability is also coherent but of opposite sign from that near the equator. Thus, while isotherms in the equatorial zone deepen, there is also a simultaneous shoaling in isotherm depth in the NECC. This second mode of variability accounts for only 18% of the field variance and is not as important as the highly coherent first mode which accounts for 49%.

3) The scale of spatial variability along the 158th meridian appears considerably different than that

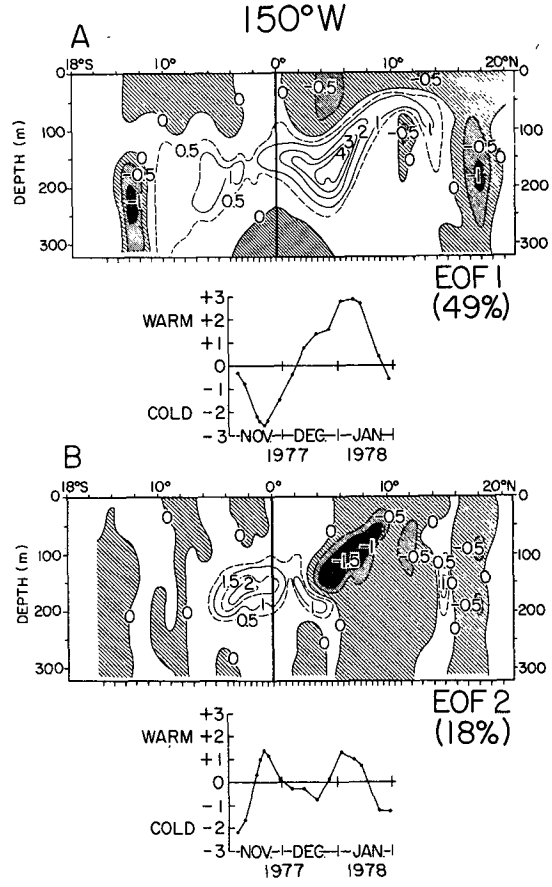

FIG. 6. The first and second principal patterns (eigenvectors) and their associated time-dependent amplitude functions for 150°W (units are °C for the eigenvectors).

along 150°W. The region of high variability within ±3° of the equator is evident (EOF 1) but the region of strong covariability between 4 and 10°N observed in the 150° section is missing. It may be noteworthy that this is the latitude range of the Line Islands which are more or less bisected by the 158th meridian (see Fig. 1 and following discussion).

4) The time character of the principal modes of variation at each longitude is characterized by time scales on the order of 2–3 months or longer. This scale is somewhat longer than expected from stability theory (e.g., Philander, 1978) and longer than the month-type scales seen from other sets of indirect measurement (e.g., Wyrtki, 1978b; Harvey and Patzert, 1976; Legeckis, 1977). The existence of an energetic 4-day oscillation in the thermal structure was not apparent in this study as evidenced by (i) the small variation in the first and second amplitude functions for 150°W during the rapid sample period in the middle of November and (ii) inspection of the individual sections obtained during the rapid sample period.

5) The structure in EOF 1 at higher latitudes, be-

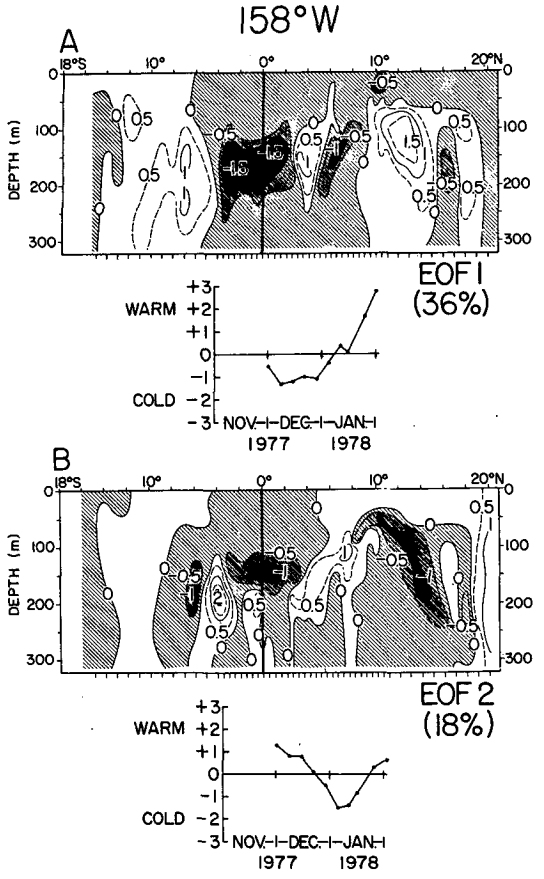

FIG. 7. As in Fig. 6 except for 158°W.

tween 14 and 20°N, at both 150 and 158°W is due largely to the eddies that moved to the west at both meridians. An example of one of these eddies in the North Equatorial Current is seen in Fig. 2. This aspect of the data set will be discussed at length elsewhere. For now, we only note that separate calculations with the eddy features removed gave identical conclusions to those stated above.

The above results could be overly influenced by two factors. The burst sample period during the end of November contributed four sections to a relatively short time series (16 terms) at 150°W. Thus one might argue that the analysis is biased toward the state of the ocean during this heavily sampled interval. A recomputation of the normal mode structure along the 150°W section excluding three of these four flights, i.e., so that the data are now approximately evenly spaced at weekly intervals, gave almost exactly the same result as shown in Fig. 6. Thus the high-density sampling did not bias the results.

A more severe criticism of the analysis could be raised since variance in the field is rather tightly confined in the vertical. Thus the analysis technique will concentrate on variability in this region excluding perhaps important events or relations existing in other parts of the water column or latitude segments of each section. This possibility was investigated in two different ways. First, the time series for each of the stations, i.e., each depth/latitude position, were normalized to have unit variance. Thus each of the 510 stations that went into the analysis contributed equally to the estimation of the EOF's. Examinations of the eigenvectors and amplitude functions that resulted from this analysis (Fig. 8A) show basically the same results as Figs. 6 and 7. As expected, the field is more smooth and featureless. However, this subsequent analysis emphasizes more strongly the large degree of covariability existing across the length and depth of the 150° section.

Another view of the data was obtained by analyzing the isotherm depth fluctuations (cf. Fig. 5) according to Eq. (1). The results of this analysis (Fig. 8B) give almost the same conclusions as above. The horizontal scales are the same and even the maxima occur at the same latitudes (4°N and 6°S). The high degree of similarity between the EOF's of isotherm displacements and temperature fluctuations suggests that the vertical gradients between ±10° re-

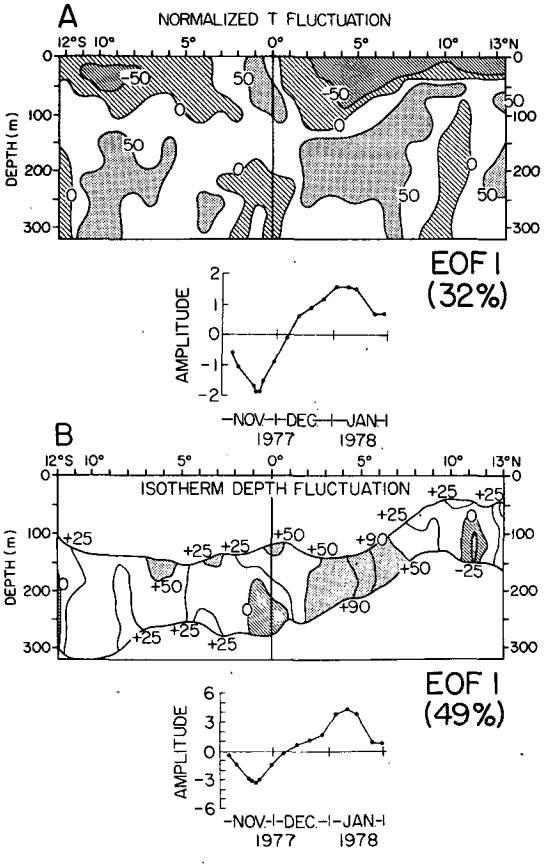

FIG. 8. The first principal component for (A) standardized temperature fluctuations and (B) isotherm depth displacement.

mained nearly constant over the course of the experiment. Thus the large-scale signal is due to vertical displacements of the entire thermal structure (cf. Wyrtki *et al.*, 1977).

We conclude that the characteristic meridional length scale associated with the variations in thermal structure that we observed along 150°W is of order 1000–2000 km. At 150°W, this coherent variation extends across the equator, through the boundaries of major equatorial currents and across the Intertropical Convergence Zone. The principal scales along 158°W are somewhat less, being of order 500 km. One possible explanation of this result is that the Line Islands may have some effect on the thermal structure in their vicinity. Such a conclusion regarding island effects is not new (e.g., White, 1971; Barkley, 1972; Patzert and Bernstein, 1976). The analysis also clearly demonstrates that the principal temporal variability associated with these large-scale spatial fluctuations is order of two months. The effect of the 4-day waves, in sampling the thermal structure of the Pacific as we have done, does not appear to be important.

Given the characteristic length and time scales associated with the EOF structure shown in Figs. 6 and 7 plus the background noise levels associated with higher modes, it should be possible to devise an appropriate sampling scheme for equatorial thermal monitoring. Simple consideration of the scales alone suggests a latitudinal separation of measurement points of ~100 km with a frequency of measurement approximately every 2–3 weeks.

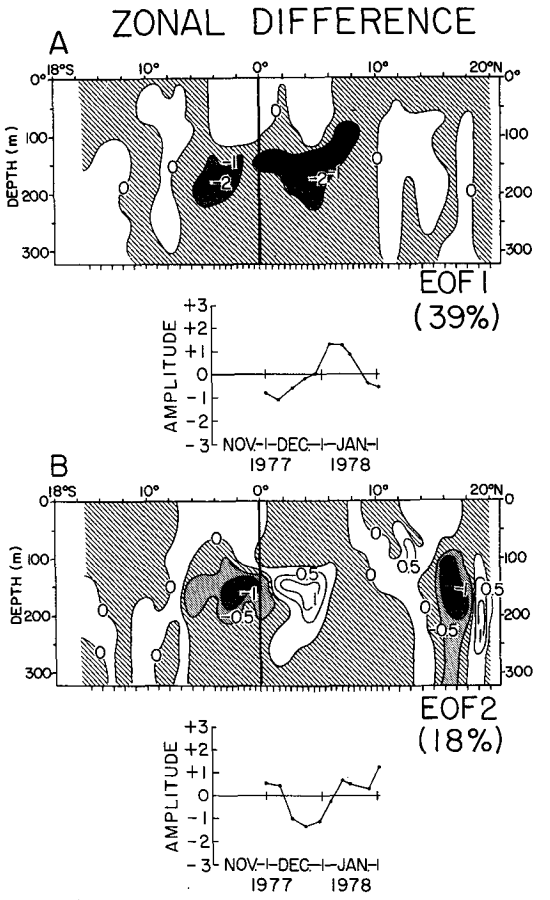

FIG. 9. The first (A) and second (B) principal patterns (eigenvector) and associated amplitude functions for the difference field obtained by subtracting the 158°W section from a "simultaneous" 150°W section (units are °C for eigenvectors).

5. Longitudinal scales of variability

To investigate variability in the east-west direction we have subtracted contemporaneous sections from each other. In doing so, we have assumed that sections, taken roughly two days apart, are for present purposes "simultaneous." The difference field represents a mixture of 1) variability that is in phase between the two longitudes but of different amplitude at each meridian and 2) variability that is out-of-phase between the two longitudes.

The resulting difference field, after removal of the mean, was represented as a set of EOF's. The first and second modes of variability, which together account for 57% of the total variance, are shown in Fig. 9. Analysis of the normalized data and isotherm depth fluctuations showed basically the same patterns.

The following conclusions may be drawn from these illustrations:

1) There is a high degree of covariability between the two meridians in the latitude range 6°S to 10°N. The sense of the variations is the same on both sides of the equator, i.e., the isotherms are either rising or deepening in unison. The second mode shows a high degree of variability within ±6° of the equator. However, variations on opposite sides of the equator are out of phase with each other.

2) The time variation of each of these modes seems to have gone through roughly one cycle over the 2-month duration of the measurements. While the data are hardly adequate to discuss periodicity, they again suggest that a time scale of order several months is appropriate to both modes of variability. This scale is again somewhat longer than expected from previous work.

3) An interesting feature of EOF 2 is observed near 17°N. Other measurements (Patzert *et al.*, 1978) show that during the two months covered by these analyses large mesoscale eddies moved from east to west at both 150 to 158°W in the North Equatorial Current. Fig. 2 shows the intense cyclonic eddy at 150°W between 15 and 20°N. Apparently, it is the passage of these eddies which is being partially observed in mode 2. However, the major variance caught by this pattern is clearly associated with the near-equatorial region.

4) The quasi-sinusoidal nature of the amplitude functions (particularly A_1) plus the high degree of coherence exhibited in the EOF's suggest some type of propagating disturbance between the two meridians. The data do not allow one to estimate a direction of propagation. In fact, we can do no more than suggest the possible occurrence of such an event based on the very limited data source.

We conclude that there is a significant east-west covariability between the two sections that were occupied. The nature of the variability was such that when the thermocline was shallower than average at one section it was deeper than average at the other section. This result suggests that a great deal of caution should be exercised in performing what might appear to be routine zonal averages of near-equator ocean temperatures, for the results may be dependent on the averaging interval. Likewise, care must be taken when inferring zonal coherence in temperature variations, for again, the result may depend critically on station location.

The time scale of zonal variation is approximately two months. This suggests an extra constraint on the temporal sampling scheme mentioned in Section 4. If indeed two months is a representative time scale of the patterns shown in Fig. 9, then a sampling interval of approximately two weeks is required for a minimum resolution. The two-month time scale also implies that some thought be given to the act of simple temporal averaging of equatorial temperature data as well as the interpretation of past, present and future hydrographic surveys of the area for they are apt to be significantly aliased.

6. Relating observed wind fields to temperature variations

a. Local wind forcing

An attempt was made to relate information on the local wind field to the characteristic temporal signatures of temperature variation (Figs. 6–9). Two different measures of the local wind were used:

1) Moored buoys with wind recorders were positioned ~100 km apart during the experiment at latitudes 6, 7 and 8°N along the 150th meridian. This vector wind data, taken every 15 min, was made available to us by David Halpern, PMEL (Halpern, 1979). Weekly averages of the u and v components were computed along with similar averages of $(u^2 + v^2)$.

The resulting time series were nearly identical for all three quantities. They showed that the zonal component increased linearly over the 14 weeks of data. The v component which was toward the north at the beginning of the experiment decreased linearly also over the 14 weeks reversing toward the south at about week 7 as the ITCZ passed over the buoy array. The squared wind speed increases slowly for the first 11 weeks and then rapidly during the last three weeks.

2) Vector wind observations were also available at 6 h intervals from the Line Islands (Christmas, Fanning and Palmyra) and Malden Island (cf. Fig. 1). The typical island separation varies from 200 to 1200 km. These data, made available by Marty Vitousek, University of Hawaii, were also converted to weekly averages of u, v and $(u^2 + v^2)$. The island winds, while not as consistent as the buoy observed winds, still showed, to first order, the same general time trends as the buoy winds.

None of the wind variables above exhibited a temporal behavior similar to those shown in Figs. 6–9. This statement includes the v component found previously by Groves and Grivel (1962) and Wunsch and Gill (1976) to be important to shorter period oceanic fluctuations. We did not feel the data were adequate to attempt calculations of $\nabla \times \tau$, etc. However, since the time trends of the components were all rather linear it is difficult to see how estimates of $\nabla \times \tau$, etc., derived from the data could be made to replicate the time behavior of the empirical modes which are more or less sinusoidal. We conclude that variations of the local wind field, on the spatial scale of the station separations listed in 1) and 2) above, cannot explain the major signals we have observed in the thermal structure.

b. Regional wind forcing

A larger scale view of the trade wind field in the central equatorial Pacific was available through the FNWC Global Band Analysis. The FNWC winds appear reasonably accurate at midlatitude (Friehe and Pazan, 1978). Their validity at lower latitudes, while generally not as good, appeared adequate during this experiment to detect any strong relation between wind forcing and thermal response (Pazan *et al.*, 1980).

The wind components at 12 h intervals were obtained over a region bounded by 140–170°W and 15°N–15°S on a grid of ~250 km. Both the magnitude of the wind stress and curl of the wind stress were computed on this grid. For present purposes it suffices to show these properties of the wind field as they vary in latitude and time at 150°W. Averages over the entire region, as well as other individual longitudes, are not greatly different than those at 150°W.

The properties of the stress field observed during the experiment are shown in Fig. 10. The right-hand curve on that illustration shows the time-averaged stress field at 2.5° latitude intervals over the 3-month period. The stress is highest near 10°N as expected and drops rapidly as one moves south. These lati-

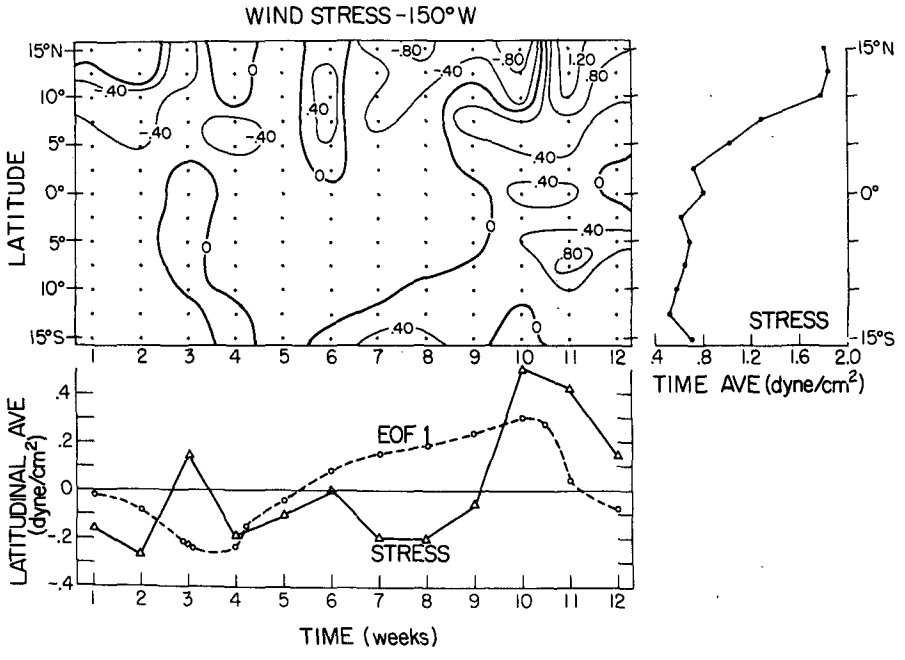

FIG. 10. Main panel: Latitude/time plot of wind stress (dynes cm^{-2}) fluctuations about time mean. Right panel: Time mean of wind stress as a function of latitude. Lower panel: Weekly wind stress averaged between 5°N and 5°S (solid) and EOF 1 of temperature field at 150°W. The latter is in relative units.

tudinal means were subtracted from the weekly average stress values to give the information on the latitude/time variation of the stress field (other panels of Fig. 10). It is seen that the stress increased sharply during the last three weeks of the experiment in the latitude band 15°N to 5°S. The time variability of the near-equatorial stress field is shown in the lower portion of Fig. 10. This is the weekly stress latitudinally averaged over the region 5°N to 5°S. Again the sharp increase in the last several weeks of the experiment is apparent. These time variations are not similar to those observed in the amplitude functions for the EOF 1 at 150°W (also shown). Other latitudinal averages gave similar results.

An identical analysis (not shown) was done on the curl of the wind stress field at 150°W. Again the results showed the temporal variability of this field over the course of the experiment did not resemble the amplitude functions of EOF 1 or EOF 2 at that longitude. Thus, we also conclude that the temporal variations of the regional curl field over the area of interest do not appear similar to those observed in the ocean's thermal field. This result, plus those of Section 5 suggest that the observed oceanic variability may be due to some type of propagating disturbance (e.g., Moore and Philander, 1976; Cane and Sarachik, 1979; McCreary, 1976). However, this speculation cannot be confirmed with the existing limited data.

7. Implied scales of variability in the Equatorial Current systems

In a recent paper Wyrtki (1978c) shows that XBT sections, when combined with average temperature/salinity relations, can be successfully used to estimate dynamic heights. The dynamic heights in turn are used to estimate oceanic transport. Wyrtki (personal communication) has used part of the AXBT data set described previously to make preliminary estimates of the relative geostrophic velocity between 6 and 8°N based on *T/S* relationships. These estimates of east-west velocity are shown in Fig. 11. They show the expected result that virtually all of the relative velocity shear is in the upper 200 m. The estimated velocities (relative to 300 db) are in good agreement with typical measurements made in the North Equatorial Countercurrent. The data also show that the relative velocity shear could change by a factor of 3 over the course of two months.

To evaluate the *T/S* derived-velocities we computed the transport, with respect to 300 db, across 150°W, again between 6 and 8°N (Fig. 12). The reason for selecting these latitudes is that David Halpern (PMEL) had moored current meter arrays located at latitudes 6, 7 and 8°N. Thus we can compare directly our estimates with those obtained from the current meters [for additional details see Halpern and Freitag (1978)]. We also estimated the total transport of the North Equatorial Countercurrent over

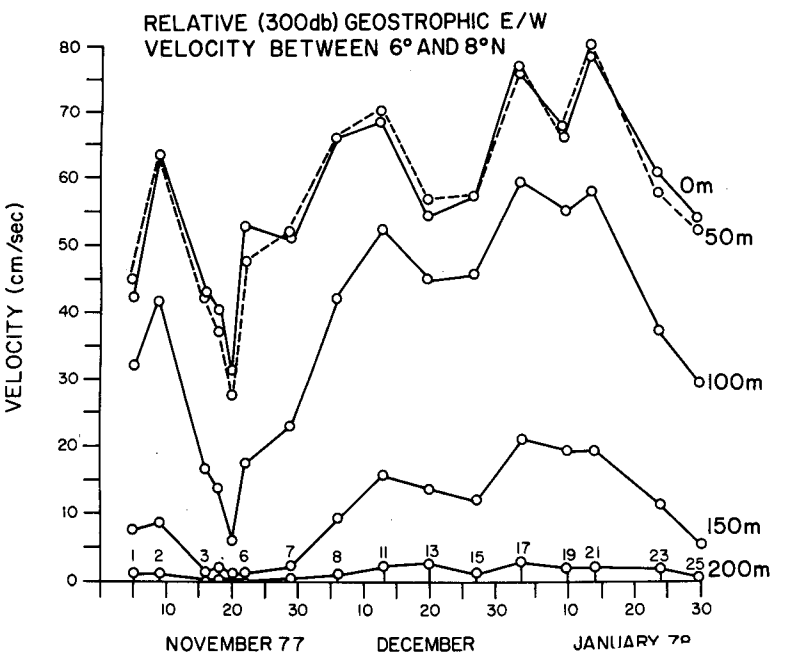

FIG. 11. Relative geostrophic east-west velocity shear (relative to 300 db) between 6 and 8°N estimated from the AXBT temperatures using *T/S* relations.

the course of the experiment and that is also shown on Fig. 12. The *T/S* derived transports are in excellent agreement with those obtained from the current meter arrays (Halpern, 1978, personal communication) and the standard hydrographic estimates (Taft and Kovala, 1979). The result noted in the previous paragraph is again clearly seen on this illustration: the total transport of the North Equatorial Countercurrent can change by a factor of 2 in a time span of approximately two months. Additional work on the

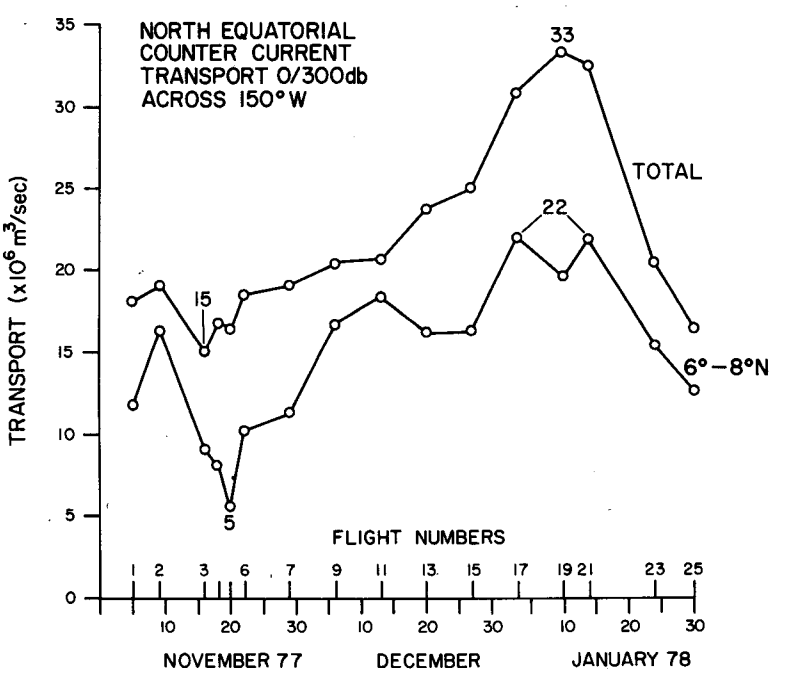

FIG. 12. The transport of the North Equatorial Countercurrent between 6 and 8°N using *T/S* relations and over the entire meridional width of the NECC current using *T/S* relations.

T/S derived transport in comparison with ship and current meter observations will be reported elsewhere.

The point of the above discussion is to show that the large-scale variations we have observed in the temperature field almost certainly occur in the velocity/transport fields, also. It may be concluded that characteristic space and time scales we have observed in the temperature field must apply in good measure to the velocity and transport fields, also. Thus, in lieu of the other information, one can use the space/time scales that have been described here for the temperature field to help design a first deployment of current meters to measure large-scale climatological fluctuations in the central Pacific Equatorial Current System.

8. Conclusions

Long-range aircraft have been used to drop AXBT's along two long meridional sections across the central equatorial Pacific. The sections were occupied approximately every week for two or three months, depending on the longitude.

Analysis of the space/time scales of the temperature section time series suggest the following principal conclusions:

1) Large-scale coherent meridional variability exists in the region within $\pm 10°$ of the equator. This coherent variability is most evident in regions of high vertical temperature gradient although it also includes both the surface layer and the deeper waters beneath the thermocline. The time scale associated with this variation is the order 2–3 months.

2) At 150°W, the large-scale variability mentioned above generally extends coherently across the equator, the boundaries between major equatorial currents, and the intertropical convergence zone. This pattern of meridional variation makes up ~50% of the variability that was observed during the course of this experiment and so, if typical, it is a major feature of the equatorial ocean.

3) Some dissimilarity between the two meridional sections exists in the latitude range of the Line Islands. This suggests that the island effects may play a predominant role in "contaminating" temperature observations in their vicinity.

4) A large-scale east-west coherence between the two sections was observed near the bottom of the mixed layer. This variation was found within 5–10° of the equator and was most intense in bands 2–6° north and south of the equator. It accounted for 39% of the total observed east-west variance. The time scale of this zonal covariability was ~2 months, a value close to the observed time scale of meridional variation. The nature of the principal patterns associated with zonal variations could be explained by some type of propagating disturbance. However, the data in this study are too limited to confirm such a hypothesis.

5) The above results should serve as a warning that block-averaging equatorial temperature data in space, particularly zonally, and time may result in substantial and undesirable side effects. The present results, if representative, suggest that much of the hydrographic data previously collected in the study area may be aliased by energetic disturbances with scales similar to those discussed above.

6) The possibility that the observed temperature variations were forced by local wind field variations was investigated using data from moored buoys, nearby islands and a large-scale measure of the trade wind field from FNWC. The results of these studies suggested that variations in the regional wind field were not responsible for a significant portion of the observed temperature change.

7) Preliminary comparisons between velocity/transport derived from *T/S* relations and actual current meter observations was excellent. This suggests that the space/time scales of variability we observed in the temperature field should apply also to the velocity/transport field.

Acknowledgments. We thank Meredith Sessions for help in obtaining data in the field, as well as for building much of the data recording equipment used in the experiment. Bernie Kilonsky and Klaus Wyrtki provided their time and facilities at the University of Hawaii to do much of the primary data conversion, error checking and reduction. Tony Tubbs carried through the EOF analyses and Steve Pazan provided the FNWC wind fields. David Halpern, Martin Vitousek, Bruce Taft and Klaus Wyrtki shared information with us that made it possible to draw the conclusion of Sections 6 and 7.

Thanks are also due to the Naval Reserve Squadrons, NOAA Research Flight Facility and the NAVOCEANO VNX8 Squadron for flying the missions. The level and quality of help provided by the plane crews from each of these facilities was excellent. Finally, our most sincere thanks to Bob Lawson (ONR) who handled the logistics, scheduling, and a myriad of other details during the course of the experiment. Without his help it would not have happened.

This work was supported as part of the NORPAX Program by National Science Foundation's International Decade of Ocean Exploration under contract NSF-OCE76-80183.

REFERENCES

Austin, T., 1960: *Symposium on the Changing Pacific Ocean, 1957 and 1958.* California Cooperative Fisheries Investigation, Vol. 7, 52–55.

Barkley, R. A., 1972: Jonston Atoll's wake. *J. Mar. Res.*, **30,** 201–216.

Cane, M. A., and E. S. Sarachik, 1979: Forced baroclinic ocean motions, III. The linear equatorial basin case. *J. Mar. Res.*, **37**, 355–398.

Friehe, C. A., and S. E. Pazan, 1978: Performance of an air-sea interaction buoy. *J. Appl. Meteor.*, **17**, 1488–1497.

Groves, G. W., 1956: Periodic variation of sea-level induced by equatorial waves in the easterlies. *Deep-Sea Res.*, **3**, 248–252.

——, and F. Grivel, 1962: Some relationships between sea level and wind in the equatorial Pacific. *Geophys. Int. Mexico*, **2**, 1–14.

Halpern, D., 1979: Surface wind measurements and low level cloud motion vectors near the Intertropical Convergence Zone in the central Pacific Ocean during November 1977 to March 1978. *Mon. Wea. Rev.*, **107**, 1525–1534.

——, and H. P. Freitag, 1978: Transport estimates of the Pacific North Equatorial Countercurrent between 6°N and 8°N along 150°W. *Trans. Amer. Geophys. Union*, **59**, 1112.

Harvey, R. R., and W. C. Patzert, 1976: Deep current measurements suggest long waves in the eastern equatorial Pacific. *Science*, **193**, 883–885.

Hires, R. I., and R. B. Montgomery, 1972: Navifacial temperature and salinity along the track from Samoa to Hawaii, 1957–1965. *J. Mar. Res.*, **30**, 177–200.

Legeckis, R., 1977: Long waves in the eastern equatorial Pacific Ocean: A view from a geostationary satellite. *Science*, **197**, 1179–1181.

McCreary, J., 1976: Eastern tropical ocean response to changing wind systems with application to El Niño. *J. Phys. Oceanogr.*, **6**, 634–645.

Meyers, G., 1978: Annual variation in the depth of 14°C in the tropical Pacific Ocean. Ph.D. thesis, University of Hawaii, 79 pp.

——, 1979: On the annual Rossby wave in the tropical North Pacific Ocean. *J. Phys. Oceanogr.*, **9**, 663–674.

Montgomery, R. G., 1969: A meridional shuttle for studying the intertropical Central Pacific Ocean. *Bull. Japan. Soc. Fish. Oceanogr.*, Special Number (Prof. Uda's Commemorative Papers), 87–90.

Moore, D. W., and S. G. H. Philander, 1976: Modeling of the tropical oceanic circulation. *The Sea*, Vol. 6, Interscience, 1048 pp. (see Chap. 8).

Patzert, W. C., and R. L. Bernstein, 1976: Eddy structure in the central South Pacific Ocean. *J. Phys. Oceanogr.*, **6**, 392–94.

——, T. P. Barnett, M. H. Sessions and B. Kilonsky, 1978: AXBT observations of tropical Pacific Ocean thermal structure during the NORPAX/Hawaii-Tahiti Shuttle Experiment November 1977 to February 1978. Scripps Institution of Oceanography, SIO Ref. Series 78024, 45 pp.

Pazan, S., T. P. Barnett, D. Halpern and A. Tubbs, 1980: Comparison of observed and model wind velocities in the equatorial Pacific. Submitted to *Mon. Wea. Rev.*

Philander, S. G. H., 1978: Instabilities of zonal equatorial currents. 2. *J. Geophys. Res.*, **83**, 3679–3682.

Preisendorfer, R. W., and T. P. Barnett, 1977: Significance tests for empirical orthogonal functions. *Preprints Fifth Conf. Probability and Statistics*, Las Vegas, Amer. Meteor. Soc., 169–172.

Taft, B. A., and P. Kovala, 1979: Temperature, salinity, thermosteric anomaly and zonal geostrophic velocity sections along 150°W from NORPAX Shuttle Experiment (1977–78). Dept. Oceanography Spec. Rep. No. 87, Ref. M79-17, University of Washington, 28 pp.

Roden, G. I., 1963: On sea level, temperature, and salinity variations in the central tropical Pacific and on Pacific Ocean islands. *J. Geophys. Res.*, **68**, 455–472.

Sessions, M. H., and T. P. Barnett, 1980: Airborne bathythermographs for oceanographic measurements. *Proc. NORDA Near Surface Ocean Experimental Technical Workshop*, Bay St. Louis, Office of Naval Research, 125–138.

White, W. B., 1971: A Rossby wake due to an island in an eastward current. *J. Phys. Oceanogr.*, **1**, 161–168.

Wunsch, C., and A. E. Gill, 1976: Observations of equatorially trapped waves in Pacific Sea level variations. *Deep-Sea Res.*, **23**, 371–390.

Wyrtki, K., 1978a: Sea level variations: Monitoring the breath of the Pacific. *Trans. Amer. Geophys. Union*, **60**, 25–27.

——, 1978b: Lateral oscillations of the Pacific equatorial countercurrent. *J. Phys. Oceanogr.*, **8**, 530–532.

——, 1978c: Monitoring the strength of equatorial currents from XBT sections and sea level. *J. Geophys. Res.*, **83**, 1935–1940.

——, G. Meyers, D. McLain and W. Patzert, 1977: Variability of the thermal structure in the central equatorial Pacific Ocean. Hawaii Institute of Geophysics, HIG-77-1, University of Hawaii, 49 pp.